Carbohydrate Polymers 364 (2025) 123742

Contents lists available at ScienceDirect

Carbohydrate Polymers

journal homepage: www.elsevier.com/locate/carbpol

The glycocalyx of *Lacticaseibacillus paracasei* NPB01 presents two different rhamnose-rich polysaccharides with non-equivalent immunomodulating activities

Samantha Armiento [a], Franca Oglio [b,c], Antonio Masino [b,c], Andrea Iovine [a], Xavier Trivelli [d], Antonio Molinaro [a,c], Yann Guerardel [e,f], Roberto Berni Canani [b,c,*], Cristina De Castro [a,*]

[a] Department of Chemical Sciences, Complesso Universitario Monte Santangelo, University of Napoli Federico II, Naples, Italy
[b] Department of Translational Medical Science, University of Naples Federico II, Naples, Italy
[c] ImmunoNutritionLab and NutriTechLab, CEINGE Advanced Biotechnologies, Naples, Italy
[d] Université Lille, CNRS, INRAE, Centrale Lille, Université d'Artois, FR 2638 - IMEC - Institut Michel-Eugène Chevreul, 59000 Lille, France
[e] Univ. Lille, CNRS, UMR 8576 - UGSF - Unité de Glycobiologie Structurale et Fonctionnelle, F-59000 Lille, France
[f] Institute for Glyco-core Research (iGCORE), Gifu University, Gifu, Japan

ARTICLE INFO

Keywords:
Capsular polysaccharide
Postbiotics
Gut barrier
Immune regulation

ABSTRACT

Lacticaseibacillus paracasei cell wall presents two capsular polysaccharides, CPS-1 and CPS-2, and a teichoic acid. CPS-1 is novel and it presents a branched heptasaccharide repeating unit, with the sequence →6)-α-D-Gal-(1→3)-β-L-Rha-(1→4)-β-D-Glc-(1→3)-α-D-GlcNAc-(1→2)-β-D-Glc-(1→6)-β-D-Glc-(1→ in the linear part to which a β-L-Rha is attached to O-4 of GlcNAc. Regarding CPS-2, its structure was previously reported for *L. casei*, and it presents the tetrasaccharide repeat 2)-α-L-Rha-(1→2)-α-L-Rha-(1→3)-α-L-Rha-(1→3)-α-D-GalNAc-(1→ as backbone, where the first Rha is substituted with a trisaccharide made of Rha, GlcNAc and Glc, and the third Rha has a Glc as a non-stoichiometric substituent. Preliminary in-vitro immunological analyses disclosed that the two glycans exert different activities. CPS-1 is superior to CPS-2 for the elicitation of IL-33, an interleukin that alerts the immune system to tissue damage or danger. CPS-2 instead is more efficient than CPS-1 in the elicitation of the antimicrobial peptides LL-37 and HBD-2, and it is a strong elicitor of occludin, a protein of the tight junctions relevant for the epithelium integrity. These findings suggest that *L. paracasei* CPSs play a synergistic and beneficial role in the gut, thus paving the way to studies aimed to examine their mode of action or their exploitation in the prevention and treatment of human gastrointestinal diseases.

1. Introduction

The human gut microbiota is a complex microbial ecosystem including bacteria, fungi, archaea, and viruses, that if playing beneficial effects for the host take the name pf probiotics. The microbiota colonises the gastro-intestinal (GI) tract across all life stages, from the infant to the elder although its composition is differently tuned across the different stages of life (Ling, Liu, Cheng, Yan, & Wu, 2022; Rodríguez et al., 2015). Bacterial polysaccharides play key roles in this process by contributing to the bacterial adaptation to the GI microenvironment and by promoting health benefits owing to their immunoregulatory properties (Garcia-Vello et al., 2020; Hidalgo-Cantabrana et al., 2012; Laplanche et al., 2025; Lee et al., 2021; Sharma et al., 2024; Verma et al., 2018). In the gut, microbial polysaccharides can be acquired by the administration of probiotics, namely of alive bacteria that are commercially available. Alternatively, microbial polysaccharides can be assumed by consumption of food (e.g. yoghurt and cheese) that is fermented with the so-call lactic acid bacteria (LAB), a group of different Gram-positive bacterial species all able to produce lactic acid by carbohydrate fermentation (Liang, Wang, Li, & Liu, 2024; Nguyen et al., 2024). In most of these cases, the bacteria are inactivated by a mild heat-treatment, and they are referred as postbiotics (Salminen et al., 2021).

Lacticaseibacillus paracasei (*L. paracasei* or LB if in images) is a member of the LAB group, it is categorized as GRAS (generally recognized as safe), and it is widely used in fermented foods and in postbiotic products (Kiousi et al., 2022), isolated from several environments, like

* Corresponding authors.
E-mail addresses: roberto.berni@unina.it (R. Berni Canani), decastro@unina.it (C. De Castro).

https://doi.org/10.1016/j.carbpol.2025.123742
Received 25 September 2024; Received in revised form 24 April 2025; Accepted 12 May 2025
Available online 14 May 2025

dairy products, plants, and human gastrointestinal tract (Smokvina et al., 2013). The consumption of foods fermented with *L. paracasei* strains is associated to beneficial effects on human health (Bengoa, Dardis, Garrote, & Abraham, 2021; Hill et al., 2018). Indeed, the dietary supplementation with a heat inactivated postbiotic deriving from cow's milk or rice fermentation with *L. paracasei* resulted in an effective protection against gastrointestinal infections in children (Oglio et al., 2022). The mechanism of this effect involves a beneficial modulation of innate and adaptative immunity (Nocerino et al., 2017) (Corsello et al., 2017), and of the gut epithelial barrier through a direct interaction with human enterocytes (Paparo et al., 2018). Another mechanism is based on the beneficial modulation of gut microbiome structure and function with increased production of the short chain fatty acid butyrate (Berni Canani et al., 2017; Roggero et al., 2020). The impact on immune response was also suggested by the significant reduction in the occurrence of allergic symptoms in Japanese students consuming milk fermented with *L. paracasei* (Enomoto, Shimizu, & Shimazu, 2006). The mechanisms of the communication processes with human cells elicited by *L. paracasei* are multiple and based on the report of closely related bacteria, these should include the interaction between the cell wall polysaccharides with the host receptors (Górska et al., 2014; Sharma et al., 2024).

The architecture of the bacterial cell wall differs between Gram-positive, as reviewed (Rohde, 2019), and it harbours a diverse range of structurally different glycans. In Gram-positive bacteria like *L. paracasei*, the cytoplasmic membrane is covered by a thick layer of peptidoglycan that serves to maintain the integrity of the bacterial cell. This layer is crossed by other glycan-containing polymers such as the teichoic acids (TA) (Brown, Santa Maria Jr., & Walker, 2013), exopolysaccharides (EPS) and/or capsular polysaccharides (CPS) (Cescutti, 2010). Typically, TA structure is given by several polyol residues, such as glycerol or ribitol, joined by phosphodiester units, further substituted with additional sugars or acyl groups. When TA is anchored to the peptidoglycan, it is termed wall TA, while if inserted into the membrane with a glycolipid portion, it is named lipoteichoic acid (Brown et al., 2013; Potekhina et al., 2011; Shiraishi, Yokota, Fukiya, & Yokota, 2016). CPS and EPS can be homopolysaccharides if made by only one type of monosaccharide, or heteropolysaccharides if assembled by different types of monosaccharides with varied linkages (Cescutti, 2010). CPS is tightly linked to the cell surface, often covalently (Tytgat & Lebeer, 2014), whereas EPS is secreted into the extracellular medium (Tytgat & Lebeer, 2014). However, it often occurs that CPS is mistaken as EPS since part of the capsule can be shed in the medium during bacterial growth. CPS and EPS have been implicated in different bacteria–host interactions with implication in the gut colonization and in the triggering of the immune response (Zeidan et al., 2017).

Based on these premises, the working hypothesis of this study is that the beneficial activities *L. paracasei* are mediated by its cell wall glycans, and that each component might have distinct effects associated. To demonstrate this hypothesis, *L. paracasei* CPSs were isolated and characterized, and their ability to prime the immune response and the healthy state of the epithelial barrier was evaluated by in vitro assays.

2. Material and methods

2.1. Bacterial culture

L. paracasei NPB-01 (DSM 34367), a Gram positive homofermentative bacterium, was stored at −80 °C in MRS broth (Oxoid, Basingstoke, UK) with 20 % glycerol. Before each fermentation, it was inoculated into fresh MRS broth (1:10) for 24 h at 37 °C, and a bacterial concentration of 10^8 CFU/mL was found at the end of the growth.

This starting culture was used as inoculum (1 % *v*/v) for fermenting 1 L of fresh MRS broth. The growth was carried out for 24 h at 37 °C and at the end of the process a concentration of 10^8 CFU/mL was found. The postbiotic was obtained inactivating the bacterium at 85 °C for 20 s and the product was stored as freeze-dried.

2.2. Bacterial cell wall polysaccharides extraction

L. paracasei polysaccharides were extracted by two different matrices, the fermented milk containing the postbiotic bacterium (heat inactivated at 85 °C for 20 s), and the bacterial biomass.

2.2.1. Isolation of the postbiotic polysaccharides

In the first approach, the dry milk powder containing the bacterium was suspended into 400 mL of Milli-Q water and centrifuged (7500 rpm, 30 min, 4 °C) to remove lactose and other oligosaccharides present in milk. This treatment was repeated four times, the supernatant discarded every time, to yield 3.89 g of biomass after freeze-drying. This pellet was assumed to contain the heat inactivated bacterium, and it was suspended in 20 mL of water plus an equal volume of *n*-butanol, and stirred at room temperature for 1 h to remove the lipoteichoic acid (Vinogradov, Sadovskaya, Cornelissen, & van Sinderen, 2015). The pellet afforded after centrifugation (9000 rpm, 15 min, 4 °C) was treated with 50 % aqueous hydrofluoric acid (HF), under stirring for 48 h at 4 °C. This procedure was adopted by assuming that the glycans were linked via a phosphodiester bridge as reported for those of other gut microbiota bacteria (Guérin, Kulakauskas, & Chapot-Chartier, 2022). The solution was neutralized with concentrated aqueous ammonia, the solid observed was removed by centrifugation (7500 rpm, 30 min, 4 °C), and the clear supernatant dialyzed against water with three changes (3500 kDa cut-off). After freeze-drying, a final yield of 0.79 mg/g of crude polysaccharide was observed.

2.2.2. Isolation of cell wall polysaccharides from the bacteria

The other approach used the pellet resulting by the bacterial growth in MRS at 37 °C for 24 h. Briefly, the pellet (2 g) was suspended in 30 mL of Milli-Q water and autoclaved (sterilizing cycle at 120 °C, 20 min). The supernatant obtained after a centrifugation (8000 rpm, 10 min, 4 °C) was filtered on a 0.45 μm filter and freeze-dried to yield 333 mg/g of crude product.

2.3. Chromatographic procedures and molecular weight (MW) evaluation

Size exclusion chromatography was performed on Sephacryl S-300 HR (1.5 × 45 cm, Cytiva 17–0599-01), packed and eluted with ammonium bicarbonate 50 mM, with the eluate monitored by a refractive index detector. Fractions were pooled, freeze-dried and analysed by proton NMR. Anion exchange chromatography on Q-Sepharose Fast Flow (1 × 1.5 mL, Cytiva 17–0510-01) was performed with a stepwise gradient of NaCl (10, 100, 200, 400, 700, 1000 mM), each eluted per three volumes of the column. The eluate corresponding to each NaCl concentration was concentrated by freeze-drying and desalted on BioGel P-10 resin (1.5 × 10.5 mL), ran in water, with the eluate monitored by a refractive index detector. Fractions were pooled, freeze-dried and analysed by proton NMR.

The molecular weight (MW) of both CPSs (CPS-1 and CPS-2) was determined via size exclusion chromatography using a TSK G-5000 PW_{XL} column (30 cm × 7.8 mm) mounted on a HPLC 1100 Agilent system equipped with a refractive index detector. NH_4HCO_3 50 mM was used as eluent at a flow rate of 0.8 mL/min. MW calibration was performed by relating the elution volume of dextran standards (5 kDa, 12 kDa, 50 kDa, 150 kDa, 410 kDa and 670 kDa, 50 μg each) to their Log_{10}MW.

2.4. GC–MS analyses

Compositional analysis was performed by transforming the glycans into the corresponding acetylated *O*-methyl glycosides, while the absolute configuration was determined by analysing the acetylated 2-octyl glycosides derived by reaction with an optically pure alcohol (*R*-(−)-2-

octanol) (De Castro, Parrilli, Holst, & Molinaro, 2010). Identification of the derivatives was inferred by GC–MS analysis by comparing the retention time of the peaks in the sample with those from in-house built standards. The monosaccharide linkage pattern was defined by the partially methylated and acetylated alditols method. Briefly, the polysaccharide was suspended in anhydrous DMSO, treated with powdered NaOH and CH_3I. The solution was extracted with water and chloroform, and the methylated polysaccharide recovered in the organic phase. The PMAA derivatives were obtained after full hydrolysis of the sample, reduction with $NaBD_4$ and acetylation, as reported (De Castro et al., 2010). Analysis of all derivatives was performed by using a GC–MS Agilent Technologies 7820 A (Santa Clara, CA, USA) equipped with a mass selective detector 5977B, an automatic injector 7693 A and a HP-5 ms capillary column (Agilent, 30 m × 0.25 mm i.d., 0.25 mm as film thickness, flow rate 1.2 mL/min, He as carrier gas). Electron impact mass spectra were recorded with ionization energy of 70 eV. The temperature program used was: 150 °C for 3 min, 150 up to 280 °C at 3 °C/min, 300 °C for 5 min.

2.5. NMR spectroscopy

2.5.1. Liquid state NMR spectroscopy

^1H and 2D NMR spectra were recorded using a Bruker AVANCE NEO 600 MHz and/or a Bruker AVANCE NEO 1.2 GHz spectrometer, equipped with 5 and 3 mm inverse cryoprobes, respectively, with gradients along the z axis. The samples were solved in 550 and 200 μL of D_2O, respectively, and the spectra were calibrated with internal acetone (δ_H = 2.225 ppm; δ_C = 31.45 ppm). For both instruments, COSY (Correlation Spectroscopy), Total Correlation Spectroscopy (TOCSY) and Nuclear Overhauser Enhancement Spectroscopy (NOESY) experiments were performed using data sets (t1 × t2) of 2048 × 512 points. Heteronuclear Single-Quantum Coherence (HSQC) and Heteronuclear Multiple Bond Correlation (HMBC), and HSQC-TOCSY experiments were performed in the ^1H-detection mode by single-quantum coherence with proton decoupling in the ^{13}C domain using data sets of 2048 × 512 points. HSQC was performed using sensitivity improvement and the phase-sensitive mode using echo/antiecho gradient selection, with multiplicity editing during the selection step (States, Haberkorn, & Ruben, 1982). HMBC was optimized on long-range coupling constants of 6–15 Hz. For transformation, the data matrix in both homo- and heteronuclear experiments was extended to 4096 × 2048 points and transformed by applying a qsine or a sine window function (Speciale et al., 2022).

Spectra of fr. A (the mixture of TA and CPS-1) were acquired at 600 MHz, at 298 K. TOCSY and NOESY and COSY experiments were acquired with 24 scans. 100 scans were recorded for HMBC and HSQC-TOCSY and 60 for HSQC experiments. Mixing time in NOESY, TOCSY and HSQC-TOCSY spectra were 200, 100 and 80 ms, respectively. For the pure CPS-1, only TOCSY and HSQC spectra were recorded to compare its data with those collected for Fr. A. CPS-2 spectra were recorded at 1.2 GHz, at 293 K. TOCSY and NOESY mixing time was set to 100 and 200 ms, respectively, and 16 scans for each one and for COSY spectrum were recorded. 128, 512 and 192 scans were acquired for HSQC, HMBC and HSQC-TOCSY spectra, respectively.

All spectra were transformed and analysed with Bruker Topspin software.

2.5.2. High-resolution magic-angle spinning (HR-MAS) NMR spectroscopy

HR-MAS NMR spectroscopy was used to investigate the molecular surface components directly on the cells (Ainsworth et al., 2014; Maes et al., 2009) by monitoring *L. paracasei* at different grow phases alive cells or after heat-inactivation (this only at the exponential phase). The bacterium was grown in MRS broth (0.5 L) and collected at various time intervals. Cells in their lag growth phase were harvested after 4 h, corresponding to an OD (optical density at 600 nm) of 0.3; cells in their early-exponential phase were harvested after 5 h, corresponding to an OD of 0.5; cells in their initial stationary phase were harvested after almost 15 h, corresponding to an OD of 3. These alive cells were recovered by centrifugation, washed with deuterated water to remove the culture medium residues. After this treatment, the pellet was suspended in a minimal amount of deuterated water and used for HR-MAS measurements. The 4-mm ZrO_2 rotors were filled with 50 μL of alive cells or with 90 μL of inactivated pellet. Monodimensional ^1H and bidimensional ^1H—^{13}C HSQC NMR experiments were performed on an 18.8 T, Avance NEO 800 MHz Bruker spectrometer, equipped with a ^1H–^{13}C-^{31}P probe with uniaxial gradients spinning at 5 kHz, at 293 K. Proton and ^{13}C magnetic field were 800 and 201 MHz, respectively. All the experiments were sourced from the Bruker library pulse programs, and delays and powers were optimized for each sample (Sadovskaya et al., 2017). All the spectral widths were 8197 Hz (^1H) with 1024 points for free induction decay resolution and 28,168 Hz (^{13}C), giving 8.0 and 220 Hz/point resolution, respectively. The spectra of *L. paracasei* cells in their lag, exponential and stationary phase, were acquired with 376, 688, and 352 scans, respectively.

2.6. Modulation of immune response and epithelial barrier in human enterocytes

2.6.1. Human enterocyte cell line

Caco-2 cells (ATCC, Middlesex, United Kingdom; accession number HTB-37) were grown in Dulbecco modified Eagle medium with a high glucose concentration (4.5 g/L) and L-glutamine, supplemented with 10 % FBS, 1 % nonessential amino acids, 1 % sodium pyruvate, and 1 % penicillin/streptomycin (Thermo Fisher Scientific). The cells were incubated at 37 °C in a humidified atmosphere containing 5 % carbon dioxide. The culture medium was changed every 2 days.

2.6.2. Human enterocytes stimulation protocol

Caco-2 cells were seeded 300.000 cells/well in a six well plate and stimulated after 15 days post-confluence with four different concentrations (1, 10, 100 and 1000 μg/mL) of the pellet of *L. paracasei* NPB01 postbiotic, or with the pure CPS-1, CPS-2, and TA for 48 h. Cells exposed to only medium were used as negative control (NT). Afterward, the cells were harvested and stored at −20 °C for further use.

The toxicity of *L. paracasei* NPB01 postbiotic, CPS-1, CPS-2, and TA assays was assessed using MTT (the bromide salt of 3-(4,5-dimethylthiazol-2-yl)- 2,5-diphenyl tetrazolium) (Sigma-Aldrich, Milan, Italy). Briefly, cells (10^4 cells/well) were seeded in 24-well plates (Corning, Inc., New York, NY, USA) with or without postbiotic at different doses (1 to 1000 μg/mL) and then incubated for 48 h at 37 °C in a 5 % CO_2 incubator. The cell viability was detected by adding 5 mg/mL of MTT solution followed by a 1 h incubation. The medium was then removed, and the converted dye was solubilized with acidic isopropanol (0.04–0.1 N HCl in absolute isopropanol). Absorbance was read at 570 nm using an Epoch Microplate Spectrophotometer (Bioteck, Winooski, VT, USA). The expression of LL-37 and occludin was determined by Quantitative Real-Time PCR. Briefly, total RNA was extracted from stimulated Caco-2 cells with TRIzol reagent (Gibco BRL, Paisley, UK). RNA samples were analysed using the NanoDrop 2000c spectrophotometer (Thermo Scientific) and purity was verified by A260/280 and A260/230 absorbance ratios. RNA reverse transcribed in cDNA with a High-Capacity RNA-to-cDNA™ Kit (Life Technologies, Waltham, MA, USA) according to the manufacturer's instructions. Complementary DNA (cDNA) was stored at −80 °C until use. Quantitative real-time PCR (qRT-PCR) analysis was performed using TaqMan Gene Expression Master Mix (Applied Biosystems, Vilnius, Lithuania) to evaluate the expression of LL-37 (Hs00189038_m1) and occludin (Hs05465837_g1). The TaqMan probes for these genes were inventoried and tested by Applied Biosystems manufacturing facility (QC). Data were analysed using the comparative threshold cycle method. We used the glucoronidase beta (GUS-B) gene to normalize the level of mRNA expression (TaqMan probes: Hs00939627_m1).

The concentrations of human β-defensin 2 (HBD-2) and IL-33 in cell supernatant were measured using specific human ELISA assay kits (Elabscience Biotechnology Inc. Wuhan, Hubei). The minimum detection concentrations were 37.5 pg/mL for HBD-2, and 9.38 pg/mL for IL-33. The ELISAs were conducted according to the manufacturer's recommendations.

2.6.3. Statistical analysis

The Kolmogorov-Smirnov test was used to determine whether variables were normally distributed. Descriptive statistics are reported as means and standard deviations for continuous variables when data were normally distributed. Differences among groups were compared by one-way ANOVA test. Differences among continuous variables, were compared by the independent sample *t*-test. Differences were considered statistically significant at $p < 0.05$. All data were collected in a dedicated database and analysed by a using GraphPad Prism 7.

3. Results

3.1. L. paracasei crude extracts from fermented milk and MRS broth

L. paracasei polysaccharides were first isolated from a commercial cow's milk powder supplement for infants, fermented with the bacterium inactivated by mild heat-treatment. The crude polysaccharide fraction was isolated in a low yield after extensive washing of the pellet with water to remove lactose and other oligosaccharides, and HF treatment at low temperature to detach the glycans attached onto the bacterial surface. After dialysis, the proton spectrum of this crude extract (Fig. 1a) reported several signals in the anomeric region (5.3–4.3 ppm), a crowded carbinolic region (4.2–3.1 ppm), and the methyl signals of acetyl groups (ca. 2 ppm) and six-deoxy monosaccharides (ca. 1.2 ppm). Of note, the different anomeric signals were present in a non-stoichiometric ratio, suggesting the presence of a heterogenous mixture.

The low yield obtained, and the complexity of the crude polysaccharide fraction led to repeat the polysaccharide isolation by using the bacterium grown in a different medium in order to dispose of higher amount of material to carry on the structural studies and to avoid the occurrence of high amounts of lactose. Hence, the *L. paracasei* grown in MRS medium was extracted by a strong heat treatment in autoclave (120 °C, 20 min), a treatment that compared to the HF hydrolysis was expected to preserve the phosphorous-containing linkages distinctive of teichoic acids while not effecting the glycosidic linkages. The proton spectrum profile of this crude product was compared to that isolated from the fermented milk (Fig. 1a,b), and it was found that the two profiles were very similar, with that from the MRS broth containing some additional signals at 1.5 and 1.3 ppm which suggested that some non-carbohydrate components produced by the bacterium were coextracted. The similarity between the HF treated postbiotic and the glycans extracted in the MRS grown biomass, named CPS-1 and CPS-2 (described in Sections 3.4 and 3.6) was later confirmed by comparing their HSQC spectra (Fig. S1).

Accordingly, the next studies were carried on the product isolated from the MRS growth due to the better yield observed (333 against 0.79 mg/cells, respectively), which provided enough material to carry on the chemical characterization and the purification procedures.

3.2. Monosaccharide composition

The monosaccharide composition of the crude product was determined by preparing the corresponding acetylated *O*-methyl glycosides (Fig. S2), while the acetylated O-octyl glycoside derivatives were analysed to evaluate their absolute configuration (Fig. S3). Rhamnose (Rha) and glucose (Glc) were the most abundant residues, followed by smaller amounts of galactose (Gal), galactosamine (GalNAc), glucosamine (GlcNAc), ribose (Rib) and glycerol (Gro) (Fig. S2a). Ribose likely derived by the nucleic acids and these were removed during the successive purification step. Regarding glycerol, it was supposed to be a component of the bacterial teichoic acid, as later demonstrated. As for absolute configuration, the comparison of the retention time of the octyl glycoside derivatives of the sample with that of the reference compounds (Fig. S3) established that all monosaccharides had the D absolute configuration, except Rha.

3.3. Size exclusion chromatography purification of the crude polysaccharide

The crude preparation underwent a first purification step by size-exclusion on Sephacryl HR-300 which gave four fractions, each labelled with a capital letter (Fig. S4a), with the first fraction (Fr. A) found blurred in the baseline of the chromatogram. The ^{1}H NMR profiles of the four fractions (Fig. 2) showed that only Frs. A and B contained polysaccharide material.

Fr. A (2 mg) displayed several signals in the anomeric region (5.2–4.2 ppm) all in a one-to-one ratio, except for the one at 4.8 ppm whose intensity was double compared to the others. Then, there was a crowded carbinolic region (4.2–3.1 ppm), one methyl at 2 ppm suggesting the presence of an acetyl group and two methyl groups at ca. 1.2 ppm diagnostic of 6-deoxy residues. Based on the pattern observed for the anomeric signals, 2D NMR studies were undertaken to establish the structure of the glycan.

As for Fr. B (13 mg), the anomeric region had a different number of anomeric protons with no stoichiometric ratio, but the presence of broad signals at ca. 0.8 ppm denoted that this sample still contained some contamination, therefore it was subjected to an additional purification

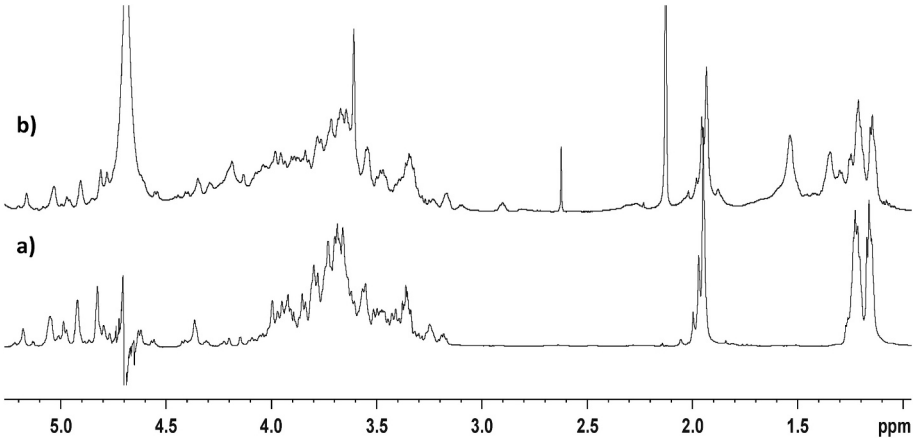

Fig. 1. ^{1}H NMR (600 MHz, 298 K, D_2O) of *L. paracasei* glycans: a) from milk matrix after HF treatment; b) from MRS, after heat treatment.

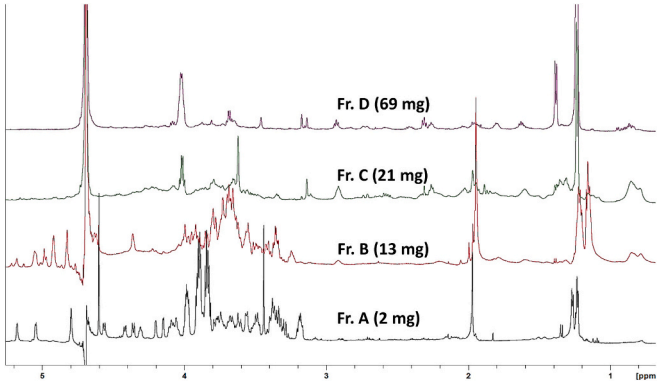

Fig. 2. Proton NMR spectra (600 MHz, 298 K, D_2O) of the fractions obtained after purification on Sephacryl HR-300. The amount isolated for each fraction is reported in brackets.

step (vide infra).

The difference between the two fractions was confirmed by monosaccharide analyses (Fig. 2Sb,c) performed after the ion exchange purification step (Section 3.5), namely on the purified polysaccharides, CPS-1 (from Fr. A) and CPS-2 (from Fr. B). In detail, Rha, Glc and GlcN were found in both glycans, while Gal was only in CPS-1 and GalN only in CPS-2 (Table S1). Regarding the ratio between the common residues, these differed consistently. Glc was the most abundant monosaccharide in CPS-1, while Rha was found as the most abundant in CPS-2 (Table S1).

3.4. NMR analysis of Fr. A

The different anomeric signals were labelled with a capital letter in order of decreasing chemical shift, and the spin system of each residue was assigned by combining the information from the complete set of the 2D NMR spectra.

Preliminary analyses focused on the anomeric region HSQC-TOCSY spectrum (Fig. 3a) which enabled the assignment of the type of residues of the sample. The anomeric proton of **A** (5.26 ppm) had four additional correlations, with one with a carbon at 54.3 ppm therefore diagnostic of the presence of an amino function. This information combined with the total number of correlations indicated that **A** was a glucosamine unit, α configured at the anomeric centre due to the value of the $^3J_{H1,H2}$ coupling constant (2.2 Hz). Similarly, the anomeric protons of **E** (4.65 ppm), **F** (4.50 ppm) and **G** (4.44 ppm) had other four correlations each, with none shifted at high field as found for **A**. Accordingly, these residues were identified as Glc units, all β configured at the anomeric centre based on the $^3J_{H1,H2}$ coupling constant measured (7.6 Hz for **E** and **F**, 7.8 Hz for **G**).

Regarding **B**, the chemical shift of the anomeric proton (5.13 ppm) was diagnostic of the α configuration of the residue in agreement with the $^3J_{H1,H2}$ value measured (3.6 Hz). In this case, the HSQC-TOCSY spectrum had three correlations with the one at ca. 70.6 ppm given by the overlap of the C-3 and C-4 densities, as later established. The presence of three correlations is diagnostic of a *galacto* configured residue, as later confirmed by the analysis of all the spectra acquired. Finally, **C** and **D** (both at 4.88 ppm with **D** slightly at lower field than **C**) only displayed one weak correlation each, a pattern diagnostic of a *manno* configured unit, in agreement with the presence of rhamnose from the

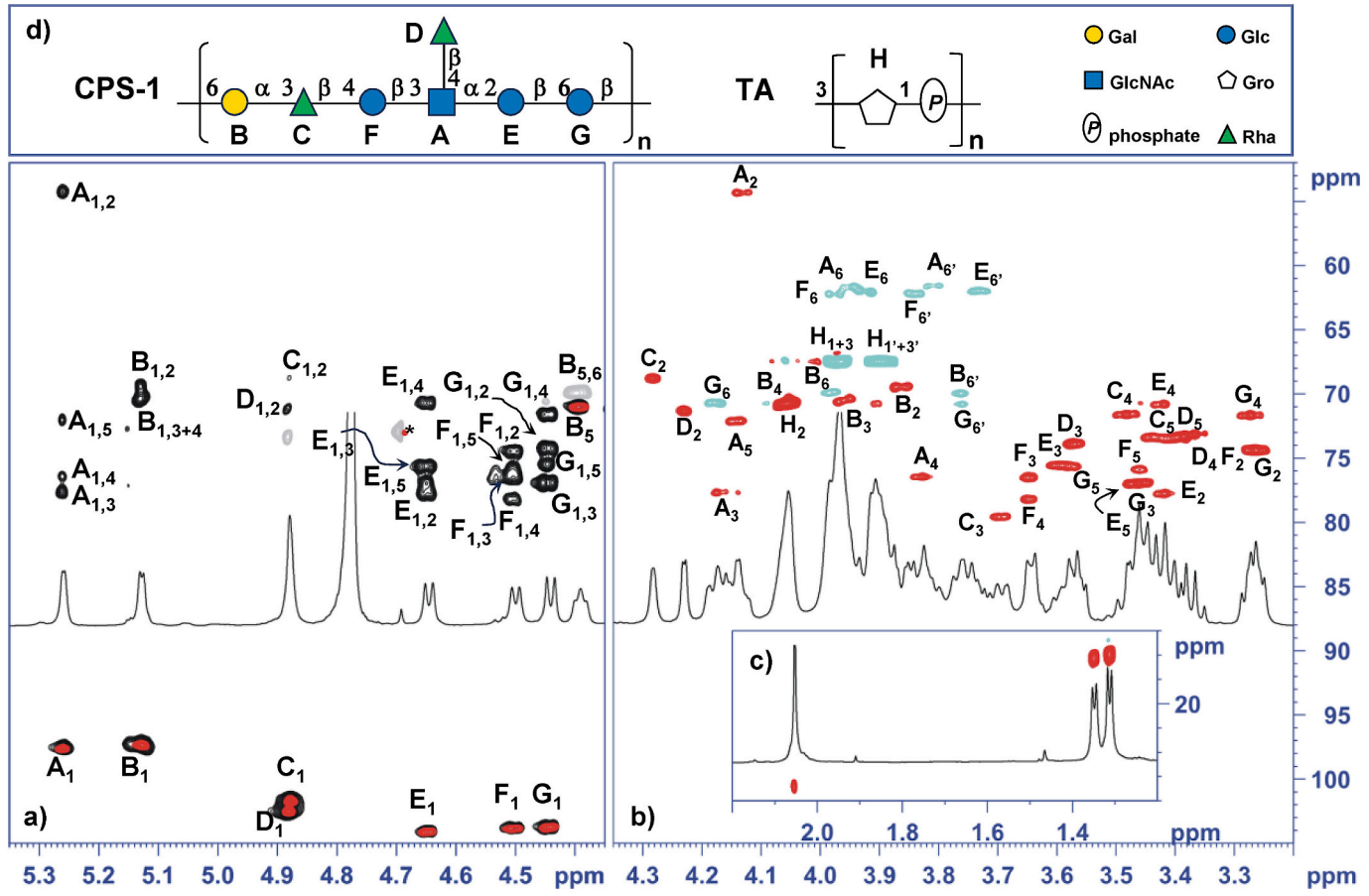

Fig. 3. HSQC-TOCSY (black/grey) and HSQC (red/cyan) spectra of Fr. A from *L. paracasei*. a) Expansion of the anomeric region of the HSQC-TOCSY spectrum overlapped with the HSQC spectrum. HSQC expansions detailing (b) the carbinolic region, and (c) the high field region. d) structures of CPS-1 and TA drawn according to the Symbolic Nomenclature of Glycans. Letters refer to the monosaccharide residues as reported in Table 1. * = impurity.

monosaccharide composition analysis.

The analysis of the COSY, TOCSY and NOESY spectra led to assign the proton chemical shifts of all the units (TOCSY spectrum in Fig. S5). As for **A**, the α-GlcNAc unit, it was found that H-2, H-3 and H-5 were almost coincident at ca. 4.15 ppm and their attribution was driven by the knowledge of the corresponding carbon atom values from the HSQC-TOCSY spectrum. The COSY spectrum related H-1 to H-2 at 4.13 ppm in turn connected to a carbon at 54.3 ppm (Fig. 3b), the low field value of H-2 suggested that the geminal amino function was acetylated, in agreement with the presence of the methyl group of an acetyl signal at $^{1}H/^{13}C$ 2.02/23.4 ppm (Fig. 3c). Then, the deshielded ^{13}C values of C-3 (77.7 ppm) and C-4 (76.5 ppm) compared to the standard values (71.9 and 70.4 ppm, respectively) denoted that **A** was glycosylated at both positions (Table 1). Regarding the β-Glc units **E**, **F**, and **G**, the respective carbinolic protons had a discrete level of overlap.

As for **E**, the analysis of the TOCSY spectrum disclosed that H-1 correlated with a large density at ca. 3.45 ppm given by the overlap of H-2, H-4 and H-5 and with another at 3.59 ppm, assigned to H-3 (Fig. S5). Here, the COSY spectrum connected H-1 to H-2 (3.42 ppm) and H-2 to H-3 (3.58 ppm) only because no other correlations were detected due to the signals' overlap. The finding of H-5 was inferred by searching the characteristic *intra*-residue H-1/H-3 and H-1/H-5 correlations characteristic of β-configured glucose in the NOESY spectrum. Indeed, H-1 had a NOE effect with H-3 (3.58 ppm, Fig. S6), with a proton at 3.45 ppm, assigned to H-5, and with a proton at 4.17 ppm, and an *inter*-residue NOE effect with a proton at 4.17 ppm later identified as H-6 of **G**. Finally, H-4 was found to overlap with H-2 at 3.42 ppm, and the ^{13}C chemical shift attribution was driven by the information of the HSQC-TOCSY spectrum. It was noted that at ^{1}H 3.42 ppm only the ^{13}C values at 70.5 and 77.7 ppm were compatible with the values detected in the HSQC-TOCSY spectrum slice from H-1 of **E** (Fig. 3). The carbon at 70.5 ppm was assigned to C-4 due to its match with the chemical shift of 70.6 reported for the corresponding methyl glucoside taken as reference. Then, the remaining signal at 77.1 ppm appeared was assigned to C-2 and its shift at lower field compared to the reference value (74.1 ppm) indicated that the corresponding hydroxyl function was glycosylated. Finally, the COSY spectrum correlated H-5 to two hydroxymethylene protons at 3.93 and 3.73 ppm, assigned to H-6 and H-6′, respectively, with the corresponding carbon atom at 61.6 ppm. Thus, **E** was identified as a 2-linked β-glucose (Table 1). By a similar approach, it was found that the two β-glucose units, **F** and **G**, were 4- and 6-linked, respectively. Regarding **C** and **D**, the anomeric protons had only the correlation with their H-2 in the TOCSY spectrum. However, by starting from the corresponding H-2, it was possible to assign the spin systems of two units by integrating the information from both COSY and TOCSY spectra, with this last displaying the full set of correlations up to the respective methyl groups. Then, the evaluation of the carbon chemical shifts determined that **C** was 3-linked while **D** was terminal, and that both units were β-configured at the anomeric centre based on the C-5 value of both units of 73.4 ppm (Speciale et al., 2022) matching that of the β-glycoside (73.6 ppm) and not that of the α anomer (69.4 ppm). As for **B**, the combined analysis of the COSY and TOCSY spectra established the position of H-2 (3.86 ppm), H-3 (3.97 ppm) and H-4 (4.05 ppm). Then, H-5 (4.40 ppm) was detected in NOESY spectrum due to the diagnostic H-4/H-5 correlation (Fig. S5), while the HSQC-TOCSY spectrum identified the corresponding C-6 value (69.9 ppm, Fig. 3a), diagnostic of a 6-linked unit, which was associated to two protons at 3.98 and 3.74 ppm in the HSQC spectrum, assigned to H-6 and H-6′, respectively (Table 1).

The inter-residue correlations were identified through the study of the and HMBC spectrum (Fig. 4a) which had the following inter-residue key correlations: $\mathbf{A_1E_2}$ (i.e. H-1 of **A** with C-2 of **E**), $\mathbf{B_1D_3}$, $\mathbf{C_1F_4}$, $\mathbf{D_1A_4}$, $\mathbf{E_1G_6}$, $\mathbf{F_1A_3}$, and $\mathbf{G_1B_6}$. The same correlations were also detected in the NOESY spectrum (Fig. S5) and this information taken together led to the identification of polysaccharide, named CPS-1 with an heptasaccharide repeating unit as reported in Fig. 3d.

Finally, the HSQC spectrum had few correlations left unassigned, the corresponding residue was labelled **H** and it was identified as a 1,3-polyglycerophosphate, namely a teichoic acid (TA), according to the comparison of the carbon and proton chemical shift values reported in literature (Kozlova, Streshinskaya, Shashkov, Evtushenko, & Naumova, 1999).

3.5. Ion exchange chromatography purification of Frs. A and B

Both fractions A and B were further purified by anion-exchange chromatography on Q-Sepharose fast-flow, eluted with a stepwise NaCl gradient. As for Fr. A, the scope was to isolate the CPS-1 and TA in pure form, while for Fr. B, the target was to increase the purity of the glycan. As expected for Fr. A, CPS-1 eluted with 10 mM NaCl eluent because being a neutral polymer (Fig. 4b). On the contrary, the anionic polymer TA eluted at a higher ionic strength (700 mM of NaCl). The identity of the purified components was ascertained by proton NMR (Fig. 4b).

Purification of Fr. B (10 mg) gave only one carbohydrate-containing product which was named CPS-2 (7 mg), eluted with 10 mM NaCl and used for the NMR and chemical studies. The MW of the two purified CPSs was evaluated by size exclusion chromatography, and it resulted to be 23.9 kDa for CPS-1 and 10.4 kDa for CPS-2 (Fig. S4b).

3.6. Structure of CPS-2

The preliminary analysis of the proton spectrum of CPS-2 revealed a complex anomeric region comprising >10 protons with a non-stoichiometric ratio, with some overlapped with the residual solvent signal, as noted by changing the temperature when recording the spectra (Fig. 5a). Such complexity was confirmed by analysing the linkage pattern of the sample (Fig. 5b) which disclosed that rhamnose was 2-, 3-, 3,4- and 2,3-linked, while glucose, galactosamine and glucosamine were terminal, 3-linked and 3,6-linked, respectively. The full set of 2D NMR spectra was recorded at 1.2 GHz at 293 K, a temperature that shifted the residual solvent signal in an area with less anomeric signals (Fig. 5a).

The attribution of the proton and carbon chemical shifts along with the connectivities determined by analysing the NOESY and HMBC spectra disclosed that the same glycan was already discovered in a different species, *Lactobacillus casei* BL23, renamed *Lacticaseibacillus casei* according the new taxonomic definition (Zheng et al., 2020), defined as a cell wall polysaccharide in the original publication (Vinogradov, Sadovskaya, Grard, & Chapot-Chartier, 2016). The identity of the two glycans was proven by comparing the two proton spectra (Fig. 6a,b) which were almost superimposable, as well as the HSQC spectra. From the structural point of view, CPS-2 is a rhamnose-rich

Table 1
(600 MHz, 298 K, D_2O) Proton (^{1}H) (plain text) and carbon (^{13}C) (italic) NMR chemical shifts of the mixture of CPS-1 and TA from *L. paracasei*. All residues are in the pyranose form.

Residue	1	2	3	4	5	6
A	5.26	4.13	4.17	3.83	4.14	3.95; 3.82
3,4-α-D-GlcNAc	*97.6*	*54.3*	*77.7*	*76.5*	*72.1*	*72.1*
B	5.13	3.86	3.97	4.05	4.40	3.98; 3.74
6-α-D-Gal	*97.5*	*69.4*	*70.5*	*70.9*	*71.2*	*69.9*
C	4.88	4.29	3.70	3.48	3.44	1.30
3-β-L-Rha	*101.7*	*68.8*	*79.5*	*71.5*	*73.4*	*17.8*
D	4.88	4.22	3.56	3.38	3.39	1.30
t-β-L-Rha	*102.5*	*71.3*	*73.9*	*73.3*	*73.4*	*17.8*
E	4.65	3.42	3.58	3.43	3.45	3.93; 3.73
2-β-D-Glc	*104.1*	*77.8*	*75.5*	*70.6*	*77.0*	*61.6*
F	4.50	3.25	3.65	3.65	3.45	3.97–3.84
4-β-D-Glc	*104.0*	*74.3*	*76.5*	*78.2*	*75.9*	*62.2*
G	4.44	3.25	3.45	3.26	3.59	4.17; 3.76
6-β-D-Glc	*103.4*	*74.4*	*77.0*	*71.6*	*75.5*	*70.7*
H	3.89; 3.96	3.89	3.89; 3.96			
P-Gro-*P*	*67.4*	*70.6*	*67.4*			

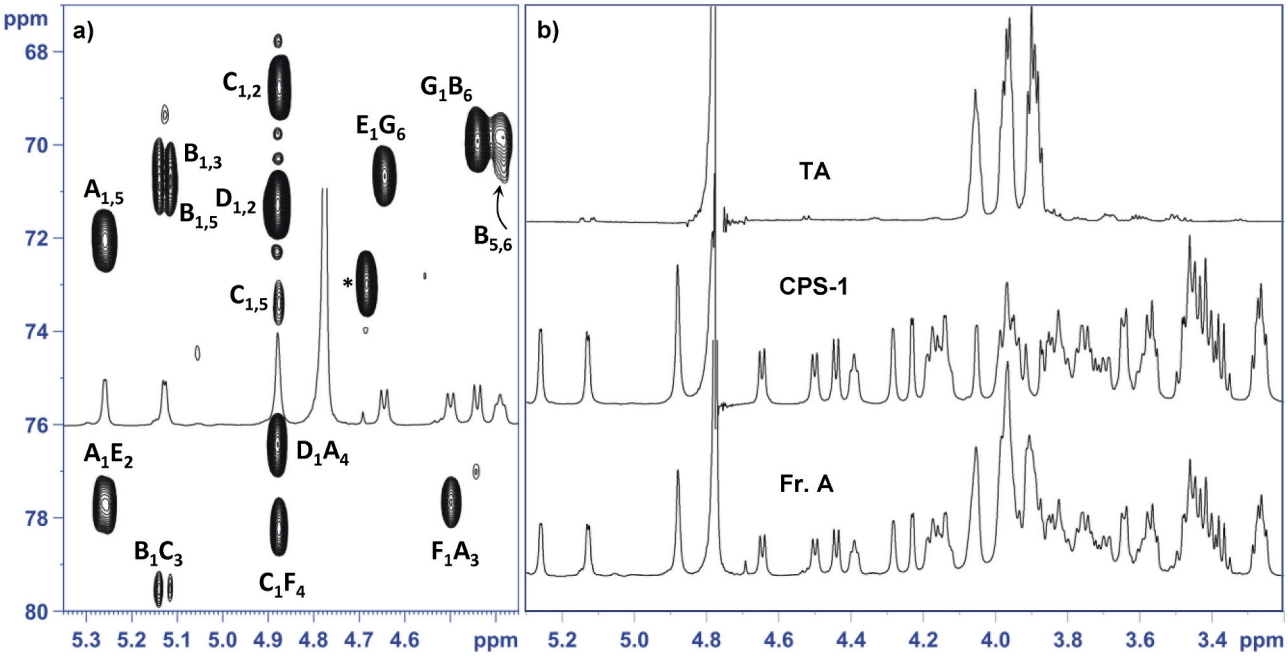

Fig. 4. a) Expansion of the HMBC spectrum of the CPS-1 isolated from *L. paracasei*, along with the proton profile and the structure. Letters refer to the monosaccharide residues as reported in Table 1. b) Comparison of the proton spectra measured for Fr. A (bottom) with the purified CPS-1 (middle) and TA (top).

polysaccharide, with all the rhamnose units α configured at the anomeric centre (Fig. 6c). The repeating unit is a branched oligosaccharide with the tetrasaccharide 2)-α-L-Rha-(1→2)-α-L-Rha-(1→3)-α-L-Rha-(1→3)-α-D-GalNAc-(1→ building the backbone, and the first Rha further substituted with a trisaccharide made of Rha, GlcNAc and Glc. Depending on the substitution pattern of the third Rha of the backbone, the repeating unit is defined as variant 1, if not further substituted, or variant 2 if it presents a α-Glc unit (Fig. 6c).

Finally, a third structural variant exists with an additional α-Glc attached to the first rhamnose. This structural motif is located at the non-reducing terminal of the polysaccharide and it considered as a termination factor of the chain (Fig. 6c) (Vinogradov et al., 2016).

3.7. HR-MAS of cell surface carbohydrates in L. paracasei

To gain information about the cell surface exposure of TA, CPS-1, and CPS-2, *L. paracasei* cells were investigated by HR-MAS NMR spectroscopy. In order disclose if the glycans presentation changed during the different *L. paracasei* growth phases, the alive bacterial cells were analysed at their late lag ($OD_{600} = 0.30$), exponential ($OD6_{00} = 0.5$) and stationary ($OD_{600} = 3$) phases. By comparison of the different HSQC spectra (Fig. 7a – c), it emerged that *L. paracasei* polysaccharides were generally more visible in the bacteria at the exponential growth phase (Fig. 7b). The low signal intensity found for the alive cells at the stationary phase was unexpected, since CPS isolation made use of bacteria at this growth stage. Accordingly, a possible explanation for this finding is that the apparent low amounts of CPSs could be an effect related to the hydrolytic enzymes expressed at this growth stage that reduced the size of the glycans, as well as mobility, so that they escaped HR-MAS detection.

Finally, the comparison of the HSQC signals of the bacterium alive cells at the exponential phase with those of the CPS-1 and CPS-2, found a match with those of CPS-2. CPS-1 and the teichoic acid were not visible, suggesting that CPS-2 was more flexible and/or more exposed on the bacterial surface and for this reason better detected by this approach.

3.8. L. paracasei glycans immune perception and epithelial barrier beneficial effects in human enterocytes

L. paracasei can be found in the human gastrointestinal tract where it is sourced mostly by milk- and/or vegetable-fermented food consumption. It is considered as a bacterium with probiotic properties able to ameliorate different pathological states, like allergy and dermatitis, and to promote the maintenance of a balanced gut microbiota along with the gut epithelium integrity.

In this frame, the effects of *L. paracasei* were evaluated on a well-validated model of human enterocytes, the Caco-2 cells. These cells were selected because display the typical features of human small intestine enterocytes and are commonly used for investigating the effects of different substances on human gut mucosa (Paparo et al., 2024).

First, to determine whether the *L. paracasei* NPB01 postbiotic, CPS-1, CPS-2, or TA were toxic to human enterocytes, cell viability was checked by MTT assay after being challenged for 48 h with the purified compounds, with concentration up to 1000 μg/mL. Since no cytotoxic effects were recorded at any dose, these compounds were deemed safe for studying their biological action in human enterocytes (Fig. S7). As biomarkers, we selected cathelicidin LL-37, human β-defensin 2 (HBD-2), occludin, and IL-33.

LL-37 and HBD-2, two antimicrobial peptides (AMPs), were selected as components of the innate immunity components because being able to exert an antimicrobial action against fungal, bacterial, and viral pathogens (Ridyard & Overhage, 2021), therefore deemed to be relevant for the maintenance of a balanced microbiota composition. Regarding occludin, this was selected as biomarker of epithelial barrier functionality since involved in the regulation of the tight junctions' network (Brunner, Ragupathy, & Borchard, 2021). Finally, IL-33 is a cytokine present in healthy intestinal tissue, but during inflammatory conditions, like inflammatory bowel disease, its expression increases to alert the immune system of tissue damage or danger, and it also plays a protective role under inflammatory conditions since it is involved in wound healing.

Dose response experiments revealed that the best effective doses for LL-37, HBD-2 and IL-33 expression were 1 μg/mL for *L. paracasei* NPB01 postbiotic, 10 μg/mL for all the other compounds (Fig. S8). Regarding

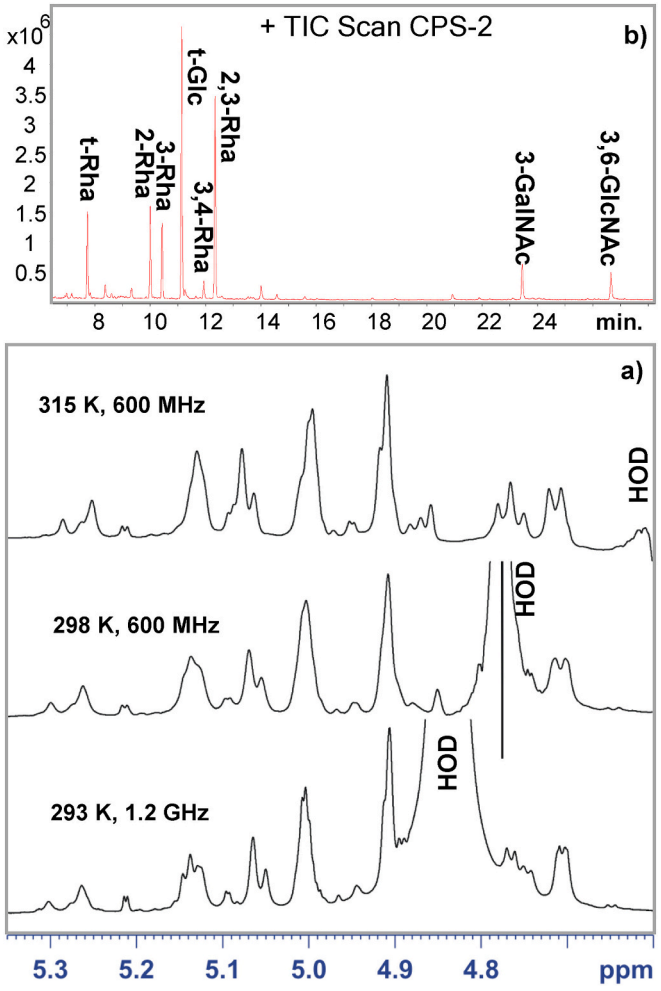

Fig. 5. a) proton spectra measured at different temperatures and at different field strength as specified on each profile, detailing the anomeric region of CPS-2. The position of the residual solvent signal is indicated with "HOD". b) GC–MS profile of the PMAA derivatives of CPS-2. The EI-MS spectra of the derivatives are reported in Fig. S6.

the regulation of occludin expression, the best effective doses were 10 μg/mL for *L. paracasei* NPB01 postbiotic, 100 μg/mL for CPS-1, 1 μg/mL for CPS-2, and 10 μg/mL for TA (Fig. S8).

Regarding the AMPs' elicitation (Fig. 8a,b), it was found that CPS-2 was very efficient in promoting the expression of LL-37, differently from CPS-1 and TA that instead did not differ significantly from the effects of the cell's medium taken as negative control. Regarding HBD-2, CPS-1 and CPS-2 had comparable and significant effects while TA was a poor elicitor but still above that of the negative control. As for occludin, CPS-2 displayed the strongest effect among all the molecules tested. Indeed, this glycan was able to promote occludin expression already at 1 μg/mL concentration while CPS-1 could trigger a similar response only if administered at 100 μg/mL concentration. Postbiotic cells lagged much behind at a 10 μg/mL concentration even though they performed better compared to TA (Fig. 8c). Regarding IL-33 production, CPS-1 had a slightly higher but significant propensity to stimulate this cytokine compared to CPS-2 and TA.

Finally, it should be noted that *L. paracasei* NBP01 postbiotic cells had in all cases an elicitation effect, which could be tentatively explained with the non-complete removal of the glycans from the bacterial surface or to the presence of other unidentified membrane components.

4. Discussion

Probiotics, particularly *Lacticaseibacillus* species, are used to improve gut health, mainly through an improvement of the microecology of the gut and the synthesis of antibacterial substances.

In this study, the working hypothesis assumed that the surface-associated bacterial glycans play a role in the activities reported, and to address this assumption, the glycans produced by *L. paracasei* were isolated and assayed in-vitro to determine their ability to trigger the innate immune response and the healthy state of the epithelial barrier.

L. paracasei is supplied as postbiotic in fermented milk, and the initial attempt to isolate these glycans from this matrix led the recovery of these molecules with a low yield due to the complex nature of the matrix. To circumvent this bottleneck, the bacterium was grown in liquid-shake culture leading to a better yield of the glycans isolated. The NMR comparison of this glycan mixture or of the purified components with that from the fermented milk demonstrated the identity between the two preparations (Figs. 1 and S1) so that the next studies were carried out on the glycans isolated from the bacterium grown in laboratory conditions.

As a result, the structure of two different polysaccharides, CPS-1 and CPS-2, and the teichoic acid was determined. CPS-1 and CPS-2 are built with a similar set of monosaccharides, except for galactose that is found only CPS-1 and GalNAc that is only in CPS-2, while they differ for their molecular weight (23.9 and 10.4 kDa, respectively, Fig. S4b) and for the structure of their repeating unit.

In CPS-1, the repeating unit is a branched heptasaccharide with a backbone made of three units of glucose, and one of rhamnose, galactose and *N*-acetylglucosamine, with this last residue branched with one rhamnose unit (Fig. 3d). Notably, both Rha units are β configured at the anomeric centre while they are α in most of the glycans, including CPS-2. The structure of CPS-1 is novel as determined by querying the Carbohydrate Structure Database (last accessed on December 2024) (Toukach & Egorova, 2016).

Differently from CPS-1, CPS-2 is not novel and it was originally described in a related species, *L. casei* (Vinogradov et al., 2016). Compared to CPS-1, CPS-2 has a higher level of ramification, the backbone is the tetrasaccharide 2)-α-L-Rha-(1→2)-α-L-Rha-(1→3)-α-L-Rha-(1→3)-α-D-GalNAc-(1→ with the first Rha always branched with a trisaccharide and the third Rha presenting a Glc as non-stoichiometric substituent (Fig. 6c). Hence, the repeat of CPS-2 is not regular as encountered in the EPS of other bacteria, mostly Gram-negative and belonging to the *Enterobacteriaceae* family, like *Hafnia alvei* (strain PCM 1189) (Katzenellenbogen et al., 2005), *Salmonella enterica* serovar Typhimurium serotype O5 (Van Puyvelde et al., 2022), and *Shigella flexneri* strain M90T (West et al., 2005). To the best of our knowledge, the CPS produced by *Ruminococcus gnavus* ATCC 35913 is the only case described so far of a Gram-positive bacterium presenting this type of structure irregularity (Laplanche et al., 2025). In this bacterium, the comparison between two CPSs that differed only for the glucosylation level, disclosed that when partially glucosylated, the CPS is more efficient in the induction of cytokines and chemokines (IL-6, CXCL1, CCL2 and IL-10) in mouse-derived bone marrow dendritic cells or in the induction of a NF-κB associated immune response in monocytes (Laplanche et al., 2025). Based on these observations, it appears that the glucosylation level can deeply affect the activities observed, although the underlying mechanism is yet to be understood.

As for the TA structure, it consists of a polyglycerol phosphate chain with no further decorations, such monosaccharide residues, like often found in many Gram-positive bacteria (Brown et al., 2013).

Concerning the biological activity, cell viability along with the regulation of mucosal immunity and gut barrier integrity were evaluated for the two CPSs and the teichoic acid and compared to the postbiotic bacterium. The teichoic acid was included in the assays due to its location on the cell membrane although not being a carbohydrate polymer itself.

First, *L. paracasei* NBP01 postbiotic, CPS-1, CPS-2 and TA resulted

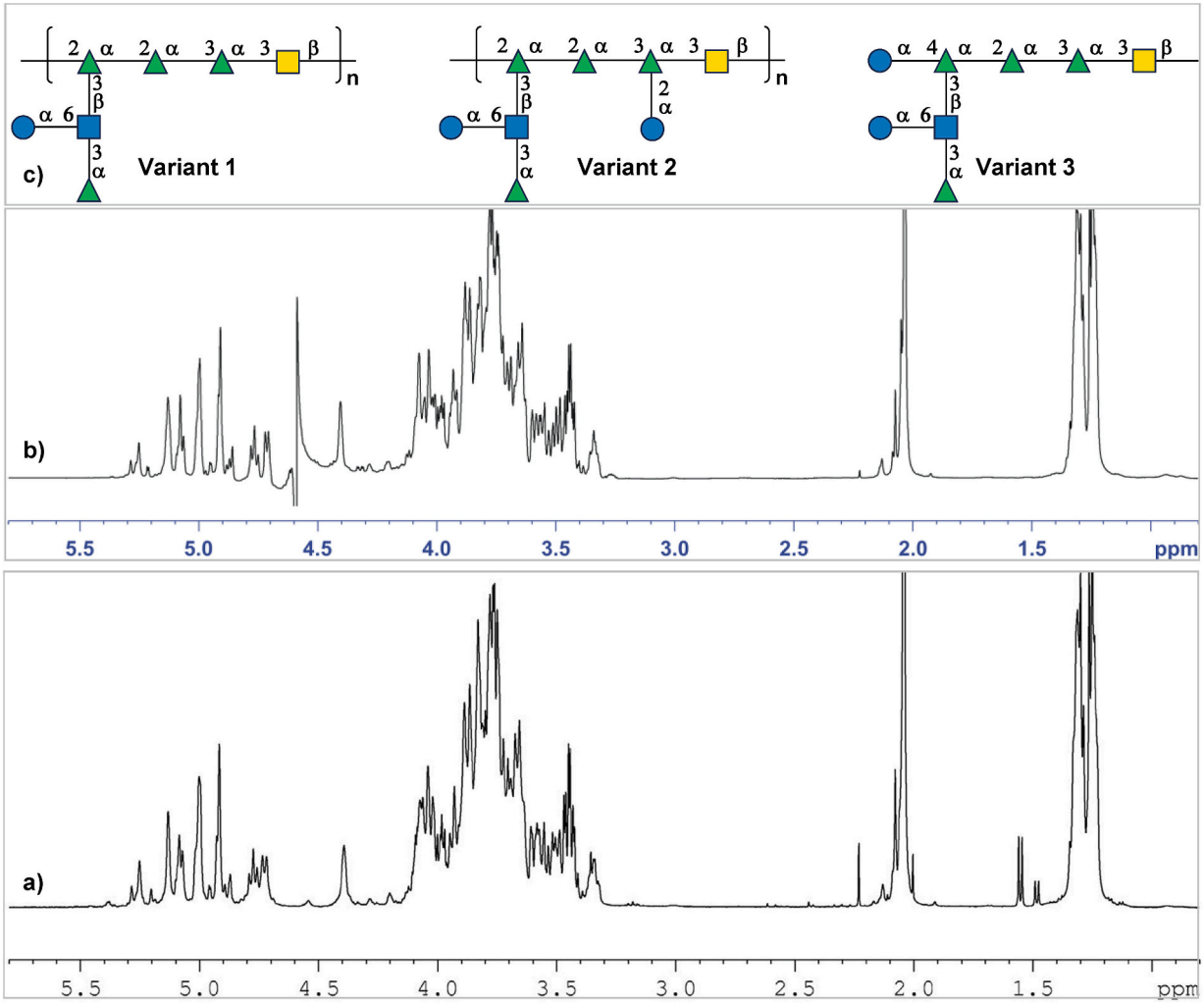

Fig. 6. ^{1}H NMR spectra of: a) *Lactobacillus casei* BL23 cell wall polysaccharide measured at 323 K at 500 MHz (Vinogradov et al., 2016); b) CPS-2 measured at 315 K at 600 MHz; c) structural motifs, defined as variants, identified in the cell wall polysaccharide of *Lactobacillus casei* BL23. The image in panel (a) is adapted from Vinogradov et al. (2016) with permission.

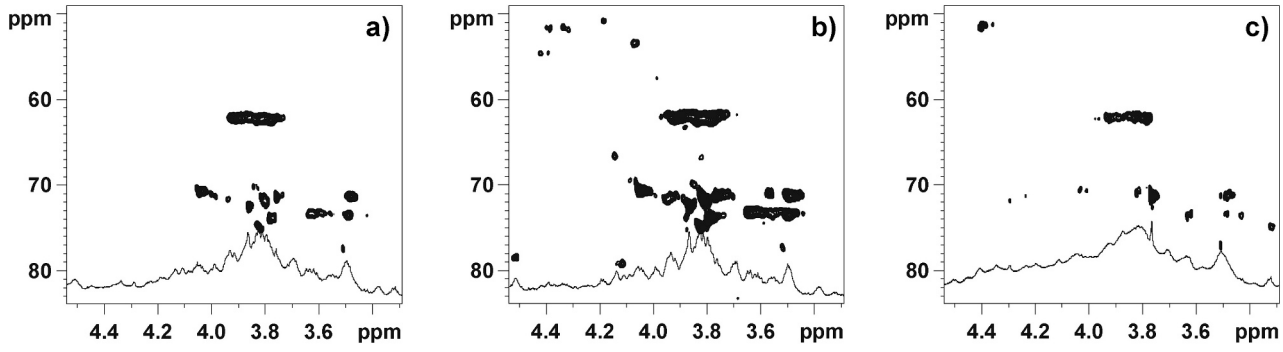

Fig. 7. (800 MHz, 293 K, D_2O) HR-MAS HSQC spectra of *L. paracasei* cells at their: a) lag; b) exponential; c) stationary growth phase.

unable to affect cell viability, confirming that all these compounds are safe for human cells. The immunomodulatory action was investigated by monitoring the expression of the antimicrobial peptides LL-37 and HBD-2.

Our research reveals that polysaccharides derived from *L. paracasei* intricately modulate the immune response within human Caco-2 enterocyte cells, showcasing a nuanced interaction between these microbial components and the host's intestinal immunity.

In particular, CPS-2 was able to increase the expression of LL-37 (Fig. 8a), a peptide of the cathelicidin family relevant in innate immunity because it is involved not only in defence mechanisms against infectious diseases, but also in the activation of human cell proliferation and migration, facilitating the wound closure process (Shaykhiev et al., 2005) and immunomodulation (Yang et al., 2020). CPS-1 did not significantly increase the expression of LL-37. HBD-2 instead is an antimicrobial peptide classified in the defensin family, active against

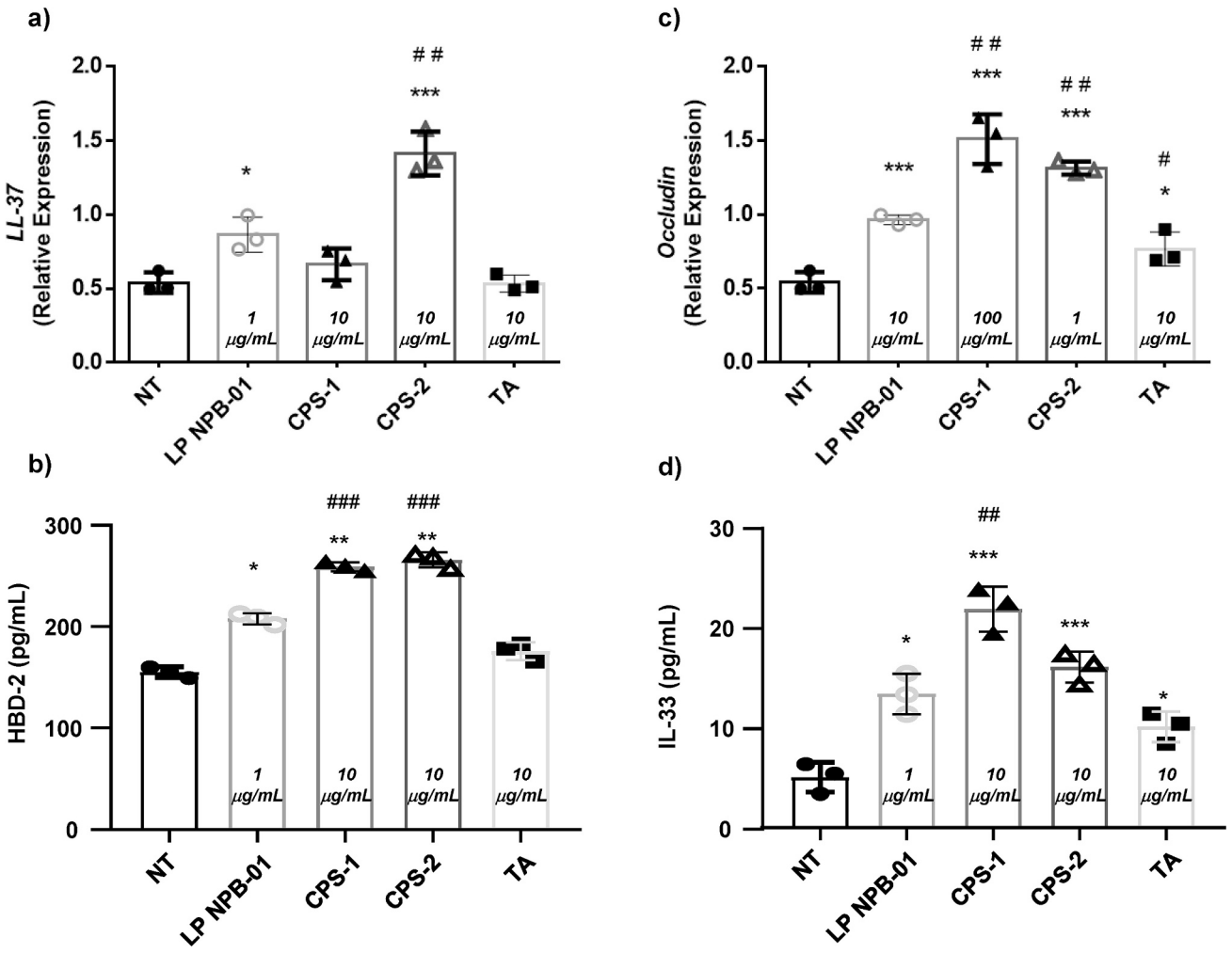

Fig. 8. Caco-2 cells stimulation for 48 h. with CPS-1, CPS-2 and TA isolated in this study. *L. paracasei* postbiotic (LP NPB-01) or cells medium (NT) were used as positive or negative control, respectively. a) cathelicidin LL-37; b) HBD-2 by human enterocytes; c) occludin; d) IL-33. The concentration of each component used to stimulate the production of the corresponding marker is indicated inside the corresponding histogram. Data were expressed as means ± SD and were analysed using nonpaired *t*-test. In panels a and b) $^{*}p < 0.05$ vs NT; $^{***}p < 0.0005$ CPS-2 vs NT, vs CPS-1 vs *L. paracasei* NPB01 postbiotic. $^{\#}p < 0.05$ TA vs *L. paracasei* NPB01 postbiotic; $^{\#\#}p < 0.005$ *CPS-1* vs *L. paracasei* NPB01 postbiotic, CPS-2 vs *L. paracasei* NPB01 postbiotic. In panels c and d) $^{*}p < 0.05$ vs NT; $^{**}p < 0.005$ CPS-1 vs NT, CPS-2 vs *NT*., $^{***}p < 0.0001$ CPS-1 and CPS-2 vs NT, $^{\#\#}p < 0.005$ CPS-1 vs LP NPB01, $^{\#\#\#}p < 0.0001$ CPS-1 and CPS-2 vs LP NPB01. Experiments were performed in triplicates and repeated 3 times.

Gram-negative bacteria, fungi and viruses, whose expression and production occurs *"on-demand"* upon challenge with Gram-negative bacteria (Schröder & Harder, 1999; Wozniak et al., 2024). Gram-positive bacteria like *Staphylococcus aureus*, *Streptococcus macedonicus* and *gallolyticus*, are considered poor elicitors of this CAMP, differently from probiotics which instead seem to have an opposite effect, as previously demonstrated for *L. paracasei*, and other lactobacilli (Schlee et al., 2008). Interestingly, a different study found that two probiotic bacteria *L. rhamnosus* and *Bifidobacterium longum*, induced the enhancement of HBD-2 production and the suppression of the regulatory factor IL-8 in an intestinal cell system challenged with *Pseudomonas aeruginosa* (Huang, Lu, & Liao, 2020). However, it should be noted that all these reports used the entire bacteria as elicitors while in this study, the enhancement of HBD-2 production points unequivocally to the bacterial CPSs.

In parallel, this study demonstrates that *L. paracasei* glycans have a modulatory action on gut barrier and on its repair mechanisms. Indeed, in human enterocytes, CPS-1 and CPS-2 stimulated occludin expression with CPS-2 being by far the component most effective between all tested, being active already at 1 µg/mL (Fig. 8c). Occludin is a key tight junction protein that is critical for maintaining the barrier function of the intestinal lining. While CPS-2 appeared as the best elicitors of the antimicrobial peptides and of the epithelium integrity, it was found that CPS-1 exerted its activity in a different context, since it was able to prime the production of IL-33, known to activate various immune cells, including mast cells, dendritic cells, and T cells, prompting the release of additional cytokines and chemokines that amplify the immune signal and recruit immune cells to the site of inflammation or injury.

Collectively, these results show that these two CPSs act synergistically on different aspects of the gut well-ness, they trigger the production of AMPs that can serve to maintain the level of the gut bacterial population, while they promote tight junction stability and barrier function of the gut epithelium or activate the repair mechanism through the IL-33 signaling.

A plausible hypothesis of the effects detected, is that glycans interact with pattern recognition receptors (PRRs) present on intestinal epithelial cells and immune cells. PRRs are a family of receptors capable of recognizing microbial-associated molecular patterns. Binding of glycans to PRRs could trigger several intracellular signaling pathways, including the NF-kB pathway, a key pathway involved in the immune response and in the regulation of gene expression of proteins crucial for the intestinal barrier function, such as occludin. Further research, such as receptor blockade experiments, transcriptomic or proteomic analyses, would be

needed to identify the specific receptors involved and the signaling pathways activated by *L. paracasei* glycans.

5. Conclusions

Overall, the findings of this study address the initial hypothesis statement, by augmenting the understanding of the complexity of the bacterial glycocalyx and by giving preliminary insights into the role of its glycans. First, *L. paracasei* is coated with two neutral CPSs, each presenting a branched structure but highly dissimilar in terms of repeating units (Figs. 3d and 6c). Second, the activities exerted by the two CPSs are not equivalent. CPS-2 is a strong inducer of occludin, thus plating an active role in the reinforcement of the gut epithelium. On the contrary, CPS-1 is superior in triggering the repair mechanisms by priming IL-33 expression. Finally, both CPSs induce the expression of HBD-2, that together with LL-37 is expected to contribute to the maintenance of the bacterial homeostasis in the gut.

In conclusion, our study has demonstrated that the two capsular polysaccharides of *L. paracasei* NBP01, CPS-1 and CPS-2, play distinct and significant roles in modulating gut immunity and barrier function. CPS-2 emerges as a potent inducer of antimicrobial peptides and epithelial integrity, while CPS-1 excels in triggering gut tissue repair mechanisms. These findings not only underscore the complexity of the bacterial glycocalyx but also highlight the potential of these polysaccharides as postbiotic compounds. Future research should focus on elucidating the precise mechanisms of action and exploring their therapeutic potential in human gastrointestinal diseases.

Glossary

AMP: antimicrobial peptide; COSY: Correlation Spectroscopy; CPS: capsular polysaccharide; DMSO: dimethyl sulfoxide; GC–MS: Gas Chromatography Mass Spectrometry; Gal: galactose; GalNAc: *N*-acetyl galactosamine; GI: gastro-intestinal; Glc: glucose; GlcNAc: *N*-acetyl-glucosamine; Gro: glycerol; HBD-2: human β-defensin 2; HF; hydrofluoric acid; HMBC: Heteronuclear Multiple Bond Correlation; HR-MAS: High-resolution magic-angle spinning; HSQC: Heteronuclear Single-quantum Coherence; IL-33: interleukin 33; LAB: lactic acid bacteria; MRS: deMan, Rogosa and Sharpe; MTT: 3-(4,5-dimethylthiazol-2-yl)-2,5-diphenyl tetrazolium bromide; NMR: Nuclear Magnetic Resonance; NOESY: Nuclear Overhauser Enhancement Spectroscopy; NT: negative control; OD: Optical Density; PRR: pattern recognition receptors; Rha: rhamnose; Rib: ribose; PMAA: partially methylated and acetylated alditol; TA: teichoic acid: TOCSY: Total Correlation Spectroscopy.

CRediT authorship contribution statement

Samantha Armiento: Writing – original draft, Methodology, Investigation, Formal analysis. **Franca Oglio:** Writing – original draft, Investigation. **Antonio Masino:** Methodology, Investigation. **Andrea Iovine:** Methodology, Investigation. **Xavier Trivelli:** Writing – review & editing, Methodology, Investigation, Formal analysis. **Antonio Molinaro:** Writing – review & editing, Methodology, Investigation, Formal analysis. **Yann Guerardel:** Writing – review & editing, Methodology, Investigation, Formal analysis. **Roberto Berni Canani:** Writing – review & editing, Visualization, Validation, Supervision, Methodology, Investigation, Formal analysis, Conceptualization. **Cristina De Castro:** Writing – review & editing, Visualization, Validation, Supervision, Methodology, Investigation, Formal analysis, Data curation, Conceptualization.

Declaration of competing interest

The authors declare that they have no known competing financial interests or personal relationships that could have appeared to influence the work reported in this paper.

The author Cristina De Castro is an Associate Editor for Carbohydrate Polymers and was not involved in the editorial review or the decision to publish this article.

Acknowledgments

AM, CDC and RBC acknowledge National Recovery and Resilience Plan (NRRP), Mission 4 Component 2 Investment 1.3 - Call for tender No. 341, Project code PE00000003, ON Foods; CN2 Agritech National Research Center and the European Union Next-Generation EU Missione 4, Componente 2, Investimento 1.4 D.D. 1032 CN00000022; POS5 Italian Ministry of Health - Health Operational Plan Trajectory 5 - Mediterranean Diet for Human Health Lab "MeDiHealthLab"; code T5-AN-07. Financial support to YG from the IR INFRANALYTICS FR2054 for conducting the research on the NMR 1.2 GHz is gratefully acknowledged.

Appendix A. Supplementary data

Supplementary data to this article can be found online at https://doi.org/10.1016/j.carbpol.2025.123742.

Data availability

Data will be made available on request.

References

Ainsworth, S., Sadovskaya, I., Vinogradov, E., Courtin, P., Guerardel, Y., Mahony, J., … van Sinderen, D. (2014). Differences in lactococcal cell wall polysaccharide structure are major determining factors in bacteriophage sensitivity. *mBio, 6*. https://doi.org/10.1128/mBio.00880-14. e00880–00814.

Bengoa, A. A., Dardis, C., Garrote, G. L., & Abraham, A. G. (2021). Health-promoting properties of *Lacticaseibacillus paracasei*: A focus on kefir isolates and exopolysaccharide-producing strains. *Foods, 10*, 2239. https://doi.org/10.3390/foods10102239

Berni Canani, R., De Filippis, F., Nocerino, R., Laiola, M., Paparo, L., Calignano, A., … Ercolini, D. (2017). Specific signatures of the gut microbiota and increased levels of butyrate in children treated with fermented cow's milk containing heat-killed *Lactobacillus paracasei* CBA L74. *Applied and Environmental Microbiology, 83*, e01206–e01217. https://doi.org/10.1128/aem.01206-17

Brown, S., Santa Maria, J. P., Jr., & Walker, S. (2013). Wall teichoic acids of gram-positive bacteria. *Annual Review of Microbiology, 67*, 313–336. https://doi.org/10.1146/annurev-micro-092412-155620

Brunner, J., Ragupathy, S., & Borchard, G. (2021). Target specific tight junction modulators. *Advanced Drug Delivery Reviews, 171*, 266–288. https://doi.org/10.1016/j.addr.2021.02.008

Cescutti, P. (2010). Chapter 6 - bacterial capsular polysaccharides and exopolysaccharides. In O. Holst, P. J. Brennan, M.v. Itzstein, & A. P. Moran (Eds.), *Microbial glycobiology* (pp. 93–108). San Diego: Academic Press. https://doi.org/10.1016/B978-0-12-374546-0.00006-7.

Corsello, G., Carta, M., Marinello, R., Picca, M., De Marco, G., Micillo, M., … Berni Canani, R. (2017). Preventive effect of cow's milk fermented with *Lactobacillus paracasei* CBA L74 on common infectious diseases in children: A multicenter randomized controlled trial. *Nutrients, 9*(7), Article 669. https://doi.org/10.3390/nu9070669

De Castro, C., Parrilli, M., Holst, O., & Molinaro, A. J. M.i.e. (2010). Microbe-associated molecular patterns in innate immunity: Extraction and chemical analysis of gram-negative bacterial lipopolysaccharides. *Methods in Enzymology, 480*, 89–115. https://doi.org/10.1016/S0076-6879(10)80005-9

Enomoto, T., Shimizu, K., & Shimazu, S. (2006). Suppression of allergy development by habitual intake of fermented milk foods, evidence from an epidemiological study. *Arerugi, 55*, 1394–1399.

Garcia-Vello, P., Sharma, G., Speciale, I., Molinaro, A., Im, S.-H., & De Castro, C. (2020). Structural features and immunological perception of the cell surface glycans of *Lactobacillus plantarum*: A novel rhamnose-rich polysaccharide and teichoic acids. *Carbohydrate Polymers, 233*, Article 115857. https://doi.org/10.1016/j.carbpol.2020.115857

Górska, S., Schwarzer, M., Jachymek, W., Srutkova, D., Brzozowska, E., Kozakova, H., & Gamian, A. (2014). Distinct immunomodulation of bone marrow-derived dendritic cell responses to Lactobacillus plantarum WCFS1 by two different polysaccharides isolated from *Lactobacillus rhamnosus* LOCK 0900. *Applied and Environmental Microbiology, 80*, 6506–6516. https://doi.org/10.1128/aem.02104-14

Guérin, H., Kulakauskas, S., & Chapot-Chartier, M.-P. (2022). Structural variations and roles of rhamnose-rich cell wall polysaccharides in Gram-positive bacteria. *Journal of Biological Chemistry, 298*, Article 102488. https://doi.org/10.1016/j.jbc.2022.102488

Hidalgo-Cantabrana, C., López, P., Gueimonde, M., de Los Reyes-Gavilán, C. G., Suárez, A., Margolles, A., & Ruas-Madiedo, P. (2012). Immune modulation capability of exopolysaccharides synthesised by lactic acid bacteria and bifidobacteria. *Probiotics and Antimicrobial Proteins, 4*, 227–237. https://doi.org/10.1007/s12602-012-9110-2

Hill, D., Sugrue, I., Tobin, C., Hill, C., Stanton, C., & Ross, R. P. (2018). The *Lactobacillus casei* group: History and health related applications. *Frontiers in Microbiology, 9*, 2107. https://doi.org/10.3389/fmicb.2018.02107

Huang, F. C., Lu, Y. T., & Liao, Y. H. (2020). Beneficial effect of probiotics on *Pseudomonas aeruginosa*-infected intestinal epithelial cells through inflammatory IL-8 and antimicrobial peptide human beta-defensin-2 modulation. *Innate Immunity, 26*, 592–600. https://doi.org/10.1177/1753425920959410

Katzenellenbogen, E., Kocharova, N. A., Zatonsky, G. V., Shashkov, A. S., Korzeniowska-Kowal, A., Gamian, A., … Knirel, Y. A. (2005). Structure of the O-polysaccharide of *Hafnia alvei* strain PCM 1189 that has hexa- to octasaccharide repeating units owing to incomplete glucosylation. *Carbohydrate Research, 340*, 263–270. https://doi.org/10.1016/j.carres.2004.11.009

Kiousi, D. E., Efstathiou, C., Tegopoulos, K., Mantzourani, I., Alexopoulos, A., Plessas, S., … Galanis, A. (2022). Genomic insight into *Lacticaseibacillus paracasei* SP5, reveals genes and gene clusters of probiotic interest and biotechnological potential. *Frontiers in Microbiology, 13*, Article 922689. https://doi.org/10.3389/fmicb.2022.922689

Kozlova, Y. I., Streshinskaya, G. M., Shashkov, A. S., Evtushenko, L. I., & Naumova, I. B. (1999). Anionic carbohydrate-containing polymers of cell walls in two streptoverticille genospecies. *Biochemistry (Moscow), 64*, 671–677.

Laplanche, V., Armiento, S., Speciale, I., Šuligoj, T., Crost, E. H., Lamprinaki, D., … Juge, N. (2025). The human gut symbiont *Ruminococcus gnavus* displays strain-specific exopolysaccharides modulating the host immune response. *Carbohydrate Polymers, 347*, Article 122754. https://doi.org/10.1016/j.carbpol.2024.122754

Lee, C., Verma, R., Byun, S., Jeun, E.-J., Kim, G.-C., Lee, S., … Im, S.-H. (2021). Structural specificities of cell surface β-glucan polysaccharides determine commensal yeast mediated immuno-modulatory activities. *Nature Communications, 12*, 3611. https://doi.org/10.1038/s41467-021-23929-9

Liang, S., Wang, X., Li, C., & Liu, L. (2024). Biological activity of lactic acid bacteria exopolysaccharides and their applications in the food and pharmaceutical industries. *Foods, 13*, 1621. https://doi.org/10.3390/foods13111621

Ling, Z., Liu, X., Cheng, Y., Yan, X., & Wu, S. (2022). Gut microbiota and aging. *Critical Reviews in Food Science and Nutrition, 62*, 3509–3534. https://doi.org/10.1080/10408398.2020.1867054

Maes, E., Mille, C., Trivelli, X., Janbon, G., Poulain, D., & Guérardel, Y. (2009). Molecular phenotyping of mannosyltransferases-deficient *Candida albicans* cells by high-resolution magic angle spinning NMR. *Journal of Biochemistry, 145*, 413–419. https://doi.org/10.1093/jb/mvp008

Nguyen, H. T., Pham, T. T., Nguyen, P. T., Le-Buanec, H., Rabetafika, H. N., & Razafindralambo, H. L. (2024). Advances in microbial exopolysaccharides: Present and future applications. *Biomolecules, 14*, 1162. https://doi.org/10.3390/biom14091162

Nocerino, R., Paparo, L., Terrin, G., Pezzella, V., Amoroso, A., Cosenza, L., … Berni Canani, R. (2017). Cow's milk and rice fermented with *Lactobacillus paracasei* CBA L74 prevent infectious diseases in children: A randomized controlled trial. *Clinical Nutrition, 36*(1), 118–125. https://doi.org/10.1016/j.clnu.2015.12.004

Oglio, F., Bruno, C., Coppola, S., De Michele, R., Masino, A., & Carucci, L. (2022). Evidence on the preventive effects of the Postbiotic derived from cow's Milk fermentation with *Lacticaseibacillus paracasei* CBA L74 against pediatric gastrointestinal infections. *Microorganisms, 11*, 10. https://doi.org/10.3390/microorganisms11010010

Paparo, L., Aitoro, R., Nocerino, R., Fierro, C., Bruno, C., & Canani, R. B. (2018). Direct effects of fermented cow's milk product with *Lactobacillus paracasei* CBA L74 on human enterocytes. *Beneficial Microbes, 9*, 165–172. https://doi.org/10.3920/bm2017.0038

Paparo, L., Coppola, S., Nocerino, R., Pisapia, L., Picariello, G., Cortese, M., … Berni Canani, R. (2024). How dietary advanced glycation end products could facilitate the occurrence of food allergy. *Journal of Allergy and Clinical Immunology, 153*(3), 742–758. https://doi.org/10.1016/j.jaci.2023.11.023

Potekhina, N. V., Streshinskaya, G. M., Tul'skaya, E. M., Kozlova, Y. I., Senchenkova, S. N., & Shashkov, A. S. (2011). Phosphate-containing cell wall polymers of bacilli. *Biochemistry (Moscow), 76*, 745–754. https://doi.org/10.1134/s0006297911070042

Ridyard, K. E., & Overhage, J. (2021). The potential of human peptide LL-37 as an antimicrobial and anti-biofilm agent. *Antibiotics, 10*, 650. https://doi.org/10.3390/antibiotics10060650

Rodríguez, J. M., Murphy, K., Stanton, C., Ross, R. P., Kober, O. I., Juge, N., … Collado, M. C. (2015). The composition of the gut microbiota throughout life, with an emphasis on early life. *Microbial Ecolology in Health and Disease, 26*, 26050. https://doi.org/10.3402/mehd.v26.26050

Roggero, P., Liotto, N., Pozzi, C., Braga, D., Troisi, J., Menis, C., … Rescigno, M. (2020). Analysis of immune, microbiota and metabolome maturation in infants in a clinical trial of *Lactobacillus paracasei* CBA L74-fermented formula. *Nature Communications, 11*, 2703. https://doi.org/10.1038/s41467-020-16582-1

Rohde, M. (2019). The gram-positive bacterial cell wall. *Microbiology Spectrum, 7*, Article GPP3-0044-2018. https://doi.org/10.1128/microbiolspec.GPP3-0044-2018

Sadovskaya, I., Vinogradov, E., Courtin, P., Armalyte, J., Meyrand, M., Giaouris, E., … Chapot-Chartier, M. P. (2017). Another brick in the wall: A rhamnan polysaccharide trapped inside peptidoglycan of *Lactococcus lactis*. *mBio, 8*(5), Article e01303–01317. https://doi.org/10.1128/mBio.01303-17

Salminen, S., Collado, M. C., Endo, A., Hill, C., Lebeer, S., Quigley, E. M. M., … Vinderola, G. (2021). The International Scientific Association of Probiotics and Prebiotics (ISAPP) consensus statement on the definition and scope of postbiotics. *Nature Reviews Gastroenterology & Hepatology, 18*, 649–667. https://doi.org/10.1038/s41575-021-00440-6

Schlee, M., Harder, J., Köten, B., Stange, E. F., Wehkamp, J., & Fellermann, K. (2008). Probiotic lactobacilli and VSL#3 induce enterocyte beta-defensin 2. *Clinican and Experimental Immunology, 151*, 528–535. https://doi.org/10.1111/j.1365-2249.2007.03587.x

Schröder, J.-M., & Harder, J. (1999). Human beta-defensin-2. *The International Journal of Biochemistry & Cell Biology, 31*, 645–651. https://doi.org/10.1016/S1357-2725(99)00013-8

Sharma, G., Sharma, A., Kim, I., Cha, D. G., Kim, S., Park, E. S., … Im, S.-H. (2024). A dietary commensal microbe enhances antitumor immunity by activating tumor macrophages to sequester iron. *Nature Immunology, 25*, 790–801. https://doi.org/10.1038/s41590-024-01816-x

Shaykhiev, R., Beißwenger, C., Kändler, K., Senske, J., Püchner, A., Damm, T., … Bals, R. (2005). Human endogenous antibiotic LL-37 stimulates airway epithelial cell proliferation and wound closure. *American Journal of Physiology - Lung Cellular and Molecular Physiology, 289*, L842–L848. https://doi.org/10.1152/ajplung.00286.2004

Shiraishi, T., Yokota, S., Fukiya, S., & Yokota, A. (2016). Structural diversity and biological significance of lipoteichoic acid in Gram-positive bacteria: Focusing on beneficial probiotic lactic acid bacteria. *Bioscience of Microbiota, Food and Health, 35*, 147–161. https://doi.org/10.12938/bmfh.2016-006

Smokvina, T., Wels, M., Polka, J., Chervaux, C., Brisse, S., Boekhorst, J., … Siezen, R. J. (2013). *Lactobacillus paracasei* comparative genomics: Towards species pan-genome definition and exploitation of diversity. *PLoS One, 8*, Article e68731. https://doi.org/10.1371/journal.pone.0068731

Speciale, I., Notaro, A., Garcia-Vello, P., Di Lorenzo, F., Armiento, S., Molinaro, A., … De Castro, C. (2022). Liquid-state NMR spectroscopy for complex carbohydrate structural analysis: A hitchhiker's guide. *Carbohydrate Polymers, 277*, Article 118885. https://doi.org/10.1016/j.carbpol.2021.118885

States, D. J., Haberkorn, R., & Ruben, D. (1982). A two-dimensional nuclear overhauser experiment with pure absorption phase in four quadrants. *Journal of Magnetic Resonance, 48*, 286–292. https://doi.org/10.1016/0022-2364(82)90279-7

Toukach, P. V., & Egorova, K. S. (2016). Carbohydrate structure database merged from bacterial, archaeal, plant and fungal parts. *Nucleic Acids Research, 44*, D1229–D1236. https://doi.org/10.1093/nar/gkv840

Tytgat, H. L., & Lebeer, S. (2014). The sweet tooth of bacteria: Common themes in bacterial glycoconjugates. *Microbiolology and Molecular Biology Reviews, 78*, 372–417. https://doi.org/10.1128/mmbr.00007-14

Van Puyvelde, S., Gasperini, G., Biggel, M., Phoba, M. F., Raso, M. M., de Block, T., … Micoli, F. (2022). Genetic and structural variation in the O-antigen of *Salmonella enterica* serovar typhimurium isolates causing bloodstream infections in the Democratic Republic of the Congo. *mBio, 13*(4), Article e0037422. https://doi.org/10.1128/mbio.00374-22

Verma, R., Lee, C., Jeun, E.-J., Yi, J., Kim, K. S., Ghosh, A., … Im, S.-H. (2018). Cell surface polysaccharides of *Bifidobacterium bifidum* induce the generation of Foxp3^{+} regulatory T cells. *Science Immunology, 3*(28), Article eaat6975. https://doi.org/10.1126/sciimmunol.aat6975

Vinogradov, E., Sadovskaya, I., Cornelissen, A., & van Sinderen, D. (2015). Structural investigation of cell wall polysaccharides of *Lactobacillus delbrueckii* subsp. bulgaricus 17. *Carbohydrate Research, 413*, 93–99. https://doi.org/10.1016/j.carres.2015.06.001

Vinogradov, E., Sadovskaya, I., Grard, T., & Chapot-Chartier, M.-P. (2016). Structural studies of the rhamnose-rich cell wall polysaccharide of *Lactobacillus casei* BL23. *Carbohydrate Research, 435*, 156–161. https://doi.org/10.1016/j.carres.2016.10.002

West, N. P., Sansonetti, P., Mounier, J., Exley, R. M., Parsot, C., Guadagnini, S., … Tang, C. M. (2005). Optimization of virulence functions through glucosylation of *Shigella* LPS. *Science, 307*, 1313–1317. https://doi.org/10.1126/science.1108472

Wozniak, W., Sechet, E., Kwon, Y.-J., Aulner, N., Navarro, L., & Sperandio, B. (2024). Identification of human host factors required for beta-defensin-2 expression in intestinal epithelial cells upon a bacterial challenge. *Scientific Reports, 14*, 15442. https://doi.org/10.1038/s41598-024-66568-y

Yang, B., Good, D., Mosaiab, T., Liu, W., Ni, G., Kaur, J., … Wei, M. Q. (2020). Significance of LL-37 on immunomodulation and disease outcome. *BioMed Research International, 2020*, Article 8349712. https://doi.org/10.1155/2020/8349712

Zeidan, A. A., Poulsen, V. K., Janzen, T., Buldo, P., Derkx, P. M. F., Øregaard, G., & Neves, A. R. (2017). Polysaccharide production by lactic acid bacteria: From genes to industrial applications. *FEMS Microbiology Reviews, 41*, S168–S200. https://doi.org/10.1093/femsre/fux017

Zheng, J., Wittouck, S., Salvetti, E., Franz, C. M. A. P., Harris, H. M. B., Mattarelli, P., … Lebeer, S. (2020). A taxonomic note on the genus *Lactobacillus*: Description of 23 novel genera, emended description of the genus *Lactobacillus Beijerinck* 1901, and union of *Lactobacillaceae* and *Leuconostocaceae*. *International Journal of Systematic and Evolutionary Microbiology, 70*, 2782–2858. https://doi.org/10.1099/ijsem.0.004107